SYNAPSE 63:421–428 (2009)

Magnetosensory Function in Rats: Localization Using Positron Emission Tomography

CLIFTON FRILOT, II,[1] SIMONA CARRUBBA,[2] AND ANDREW A. MARINO[3]*
[1]*School of Allied Health Professions, LSU Health Sciences Center-Shreveport, Louisiana 71130-3932*
[2]*Department of Orthopaedic Surgery, LSU Health Sciences Center-Shreveport, Louisiana 71130-3932*
[3]*Department of Orthopaedic Surgery, LSU Health Sciences Center-Shreveport, Shreveport, Louisiana 71130-3932*

KEY WORDS small animal imaging; electromagnetic fields; nonlinear analysis; cerebellum; evoked potentials

ABSTRACT The aim of this study was to show that low-strength electromagnetic fields (EMFs) produced evoked potentials in rats and to localize the activated region in the brain. In response to a 2.5-G, 60-Hz stimulus, onset- and offset-evoked potentials were detected ($P < 0.05$ in each of the 10 animals studied); the evoked potentials had the same magnitude, latency, and nonlinear relationship to the field seen in previous studies on rabbits and human subjects. The neuroanatomical region of activation associated with the electrophysiological effect was identified by positron emission tomography using fluorodeoxyglucose. Paired emission scans (the same animal with and without field treatment) from 10 additional rats were differenced and averaged to produce a *t*-statistic image using the pooled variance; the *t* value of each voxel was compared with a calculated critical *t* value to identify the activated voxels ($P < 0.05$). A brain volume of 13 mm^3 (15 voxels) located in the posterior, central cerebellum was found to have been activated by exposure to the field. Taken together, the results indicated that magnetosensory evoked potentials in the rats were associated with increased glucose utilization in the cerebellum, thereby supporting earlier evidence that EMF transduction occurred in the brain. **Synapse 63:421–428, 2009.**

INTRODUCTION

Electromagnetic fields (EMFs) emanating from man-made electrical devices, such as mobile phones, powerlines, and radar, are ubiquitous in the environment. Associations have been reported between brain cancer and chronic exposure to environmental EMFs (Berg et al., 2006; Villeneuve et al., 2002), but there is no agreement on the scope and extent of the risk to public health (O'Carroll and Henshaw, 2008).

One objection to the hypothesis of a causal link between the exposure and the disease is the absence of a mechanistic explanation (Olden, 1999). We proposed that the fields were transduced by the nervous system like other stimuli (Sonnier and Marino, 2001), and we presented evidence from rabbit (Marino et al., 2002) and human (Carrubba et al., 2007) studies that indicated EMF detection resulted in changes in brain electrical activity similar to those triggered by ordinary stimuli, such as light, sound, and touch. The transduction site appeared to be in the brain (Marino et al., 2003).

Our aim was to extend the results of our previous electrophysiological studies to another animal species and to localize the activated region in the brain. First, we showed that EMFs produced onset- and offset-evoked potentials in rats. Then we used positron emission tomography (PET) to identify the part of the brain that subserved transduction of the electromagnetic stimulus.

MATERIALS AND METHODS

Animals

Female Sprague-Dawley rats (approximately 300 g) were exposed to a magnetic field of 2.5 G (25 μT), 60 Hz, produced by multiturn square coils; fields having the same strength and frequency occur in the general environment (2.5 G is 3–4 orders smaller than the fields used in magnetic resonance imaging or trans-

*Correspondence to: Andrew A. Marino, Department of Orthopaedic Surgery, LSU Health Sciences Center-Shreveport, Shreveport, Louisiana 71130-3932, USA. E-mail: amarino@lsuhsc.edu

Received 3 July 2008; Accepted 26 August 2008

DOI 10.1002/syn.20619

Published online in Wiley InterScience (www.interscience.wiley.com).

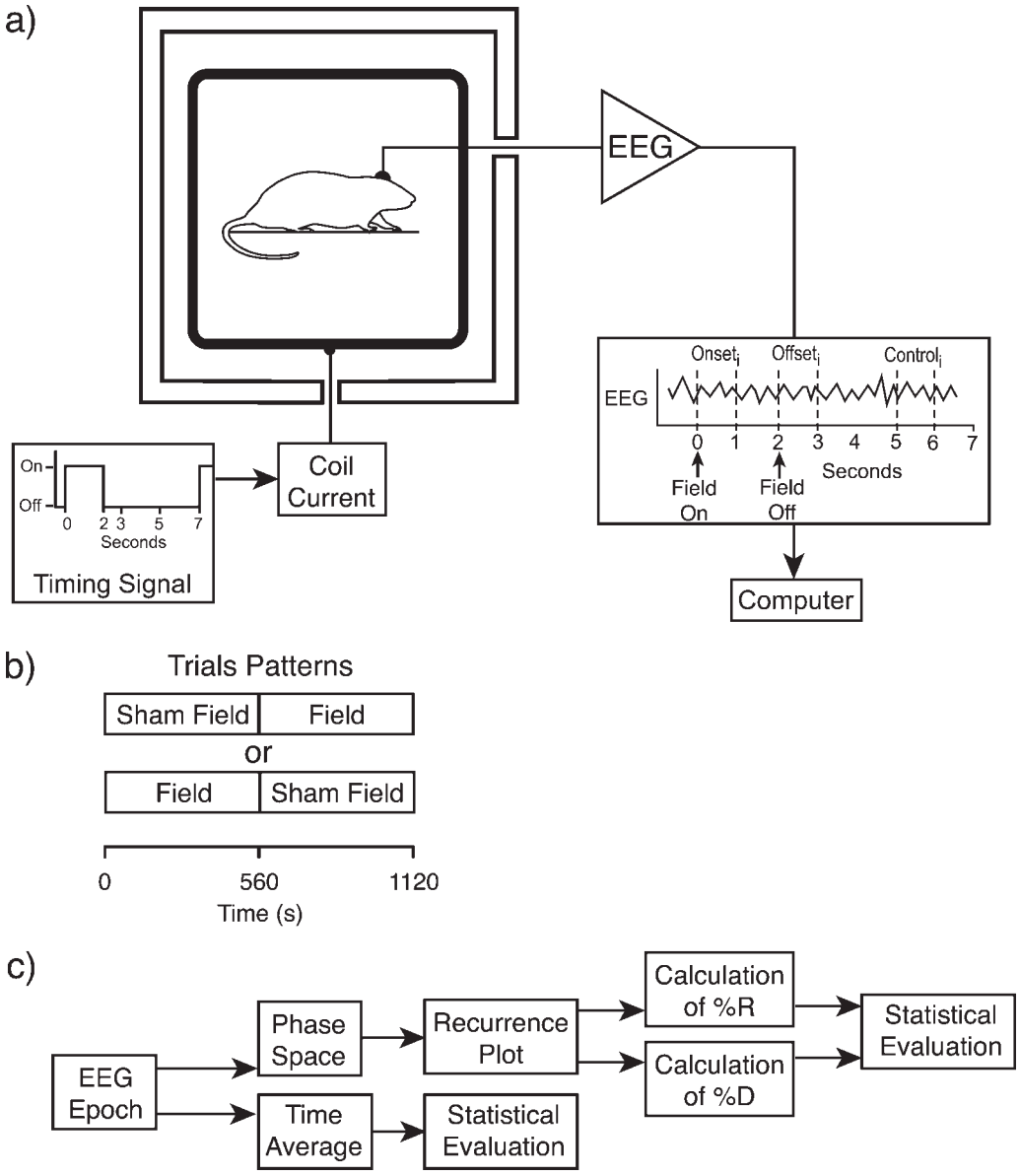

Fig. 1. Application and detection of magnetic fields. (**a**) Schematic representation of the experimental system. (**b**) Organization of trials in an experimental session. (**c**) Analytical procedures (nonlinear and linear analysis) for detecting changes in the EEG due to magnetic fields.

cranial stimulation). The coil current was regulated using a custom computer code; the resulting fields were uniform to within 10% throughout the region occupied by the rats. They were not aware of the presence of the field, as judged by the absence of behavioral responses when it was turned on or off. In the electrophysiology study, the field was applied in the coronal plane and the rats were restrained but unanesthetized (Fig. 1a). Before the experimental session, each rat was accommodated to the restraint device by means of daily practice sessions until the device was accepted with no manifestations of discomfort. In the PET study, the rats were confined in a nonmetallic cage ($28 \times 18 \times 13$ cm^3) for the duration of the 45-min exposure period (see later), but their movement in the cage was unrestricted. All field exposures took place in a darkened room; the equipment that generated and controlled the magnetic field produced no auditory or visual clues to the rat. The background 60-Hz magnetic field (present when no experimental magnetic field was applied) was 0.1 mG (0.025 μT).

Electrophysiology

Data acquisition

The EEG was recorded using a Ag/AgCl electrode (Tyco, Mansfield, MA) on top of the head and another in the middle of the back. Electrode impedances (measured before and after each experiment) were <100 kΩ. The signal was amplified (Nihon Kohden, Irvine, CA), filtered to pass 0.5–35 Hz, sampled at 300 Hz (National Instruments, Austin, TX), and analyzed offline.

Our goal was to detect the onset and offset magnetosensory evoked potentials (MEPs) caused by the field. To avoid confounding the two putative effects, the field was applied for 2 s with a 5-s interstimulus period. The EEG signal, V(t), was divided into consecutive 7-s intervals (trials) with field onset at $t = 0$ and field offset at $t = 2$ s; a portion of the interstimulus period ($2 < t \leq 7$ s) served as the control. Trials containing artifacts (as assessed by visual inspection) were discarded (<5% of all trials). The artifact-free trials were digitally filtered between 0.5 and 35 Hz after removal of the spikes (30 ms) in the EEG signal that arose from turning on or off the field (Carrubba et al., 2007). Each rat underwent two blocks of trials (80 trials/block); the field was applied during the first or second block, as determined randomly from animal to animal (Fig. 1b). The data from the block where the field was not applied were analyzed as a negative control (sham exposure). All results were determined using data from at least 50 trials.

Data analysis

Brain potentials evoked by magnetic fields can be detected by a nonlinear technique known as recurrence analysis (Carrubba et al., 2007); a detailed description of the procedure is given elsewhere (Carrubba et al., 2006). Briefly, the first 100 ms of each $V(t)$ epoch of interest (see later) was embedded in a five-dimensional phase space using a time delay of 5 points, and the corresponding recurrence plot was generated (Eckmann et al., 1987) (scale, 15%) and quantified using two variables: (1) percent recurrence ($\%R$), defined as the number of recurrent points in the plot divided by the total number of points in the recurrence matrix; (2) percent determinism ($\%D$), defined as the fraction of the points in the recurrence plot that formed diagonal lines (Zbilut and Webber, 2006). The process was repeated using a sliding window of 1 point in $V(t)$, yielding the time series $\%R(t)$ and $\%D(t)$, which were smoothed using a 100-ms, step-1 averaging window; the resulting recurrence time series $\overline{\%R(t)}$ and $\overline{\%D(t)}$ were analyzed for the presence of evoked potentials (Fig. 1c).

The expected latency range was identified by analyzing the results in the first 3 rats; we found that the evoked potentials occurred in the two recurrence time series at 200–525 ms (98 points) after presentation of the field (onset or offset), which corresponded to 100–625 ms in $V(t)$ because of the mathematical procedure used to calculate the recurrence variables (Carrubba et al., 2008). We therefore defined the epochs of interest in $V(t)$ to be $t = 0.03$–1 s, 2.03–3 s, and 5.03–6 s, which were defined to be the onset, offset, and control epochs in each trial, respectively (Fig. 1a).

Proceeding point by point, we used paired t-tests to compare the onset and control epochs, and the offset and control epochs; both comparisons were performed for each of the two recurrence time series. The probability of 10 significant tests at a comparison-wise error rate of 0.05 in 98 tests is $P = 0.0249$. We planned to conclude that the rat had exhibited an evoked potential if a significant result was observed in either $\overline{\%R}$ or $\overline{\%D}$; the corresponding family-wise error rate was therefore $1 - (1 - 0.0249)^2 = 0.049$. We evaluated the reliability of this statistical design by analyzing the sham-exposure data to empirically determine the likelihood of a false-positive decision regarding detection.

To determine whether the effect of the field could be detected by linear analysis of the EEG, the comparisons described above were repeated using $V(t)$ directly (no embedding). In each trial, $V(t)$ was averaged over the onset epoch $\left(V_{\mathrm{RMS}} = \left[\sum_{i=1}^{300} V_i^2/300\right]^{1/2}\right)$, and the resulting values were compared with the corresponding values from the control epochs to test for the presence of linear effects. The offset epoch was analyzed similarly. We planned to regard a change in brain electrical activity as nonlinear if it was detected in $\overline{\%R}$ or $\overline{\%D}$ but not in $V(t)$.

PET study

Data acquisition

The rats were injected within 15 s (injection volume, 0.5 ml) in the tail vein with 11 MBq (±10%) of ^{18}F-labeled fluorodeoxyglucose (FDG); either magnetic-field or sham-field exposure commenced immediately thereafter and continued for 45 min. Each rat was injected and scanned twice: once after field exposure and once after sham-field exposure (control). The order of the conditions was counterbalanced in the test group; the minimum time between the two PET measurements was 2 days.

By hypothesis, each onset and offset of the field triggered a magnetosensory evoked potential that increased FDG uptake, compared with sham-field exposure. To detect the putative increased uptake, the rats were anesthetized (5% isoflurane) and emission scans were obtained in 15 min in a PET tomograph (Concorde microPET, Knoxville, TN). The sinograms were corrected for scattered radiation and attenua-

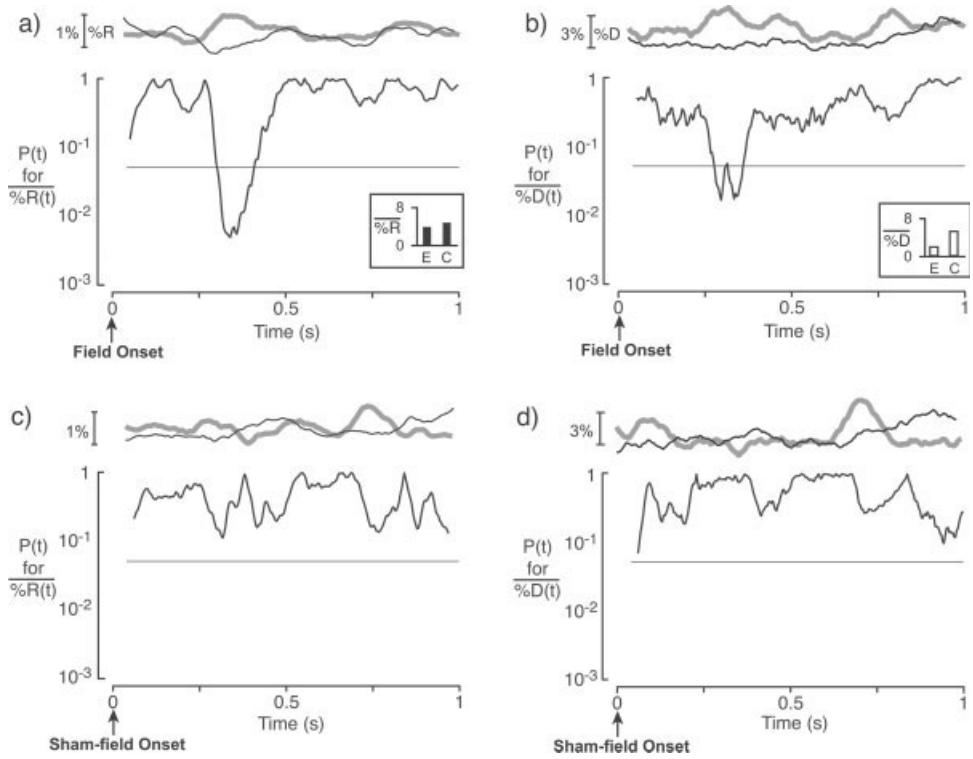

Fig. 2. Effect of magnetic-field onset on brain electrical activity of rat no. 1. (**a, b**) average value of $\overline{\%R(t)}$ ($\overline{\%D(t)}$) for the onset (black curve) and control (gray curve) epochs, and point-by-point comparison-wise probability of a difference between the two curves, assessed using the pair t-test. (**c, d**), corresponding results following sham onset. Solid line, $P = 0.05$. All curves are shown after use of a 30-point smoothing window. The average value of the recurrence variables in the onset and control epochs (E and C, respectively) in the time intervals where the epochs differed ($P < 0.05$) are given in the bar graphs. The SEs were not resolved at the scale shown.

tion, and PET images were generated using a standard filtered back-projection algorithm. The image matrices were 128 × 128 pixels with a pixel size of 0.85 × 0.85 mm^2; the spatial resolution in the axial direction was 1.21 mm (63 pixels).

Data analysis

The images were aligned (12-parameter affine transformation, with the normalized mutual information as the cost function), spatially normalized to the average of all the scans, and smoothed in all dimensions (FWHM, 2 mm). A paired analysis of the two field conditions (exposure and control) was performed as follows (Shimoji et al., 2004; Worsley et al., 1992). Each image was normalized to its mean and thresholded at 150% to separate brain and nonbrain regions. The paired images were subtracted to form difference images which were averaged across all 10 rats to create the mean difference image. The activated region was identified by calculating the image variance (t-map) and analyzing it to find the voxels for which the t value was greater than a predetermined critical value (Worsley et al., 1992). The Euler characteristic of the t-map was used to estimate the number of isolated regions of activation (Worsley et al., 1992). Statistically significant voxels in the PET images were identified by localizing their coordinates in a rat brain atlas (Schweinhardt et al., 2003).

As a negative control for the analysis, after the images were normalized the voxel values were randomized before forming the difference images. The average difference image was then evaluated as previously, resulting in a determination of the critical value of t. The process was repeated 100 times to assess the empirical probability that the critical value of t calculated from the experimental data could have been achieved by chance.

RESULTS

The rats exhibited MEPs similar in magnitude, latency, and dynamical origin to those exhibited by rabbits (Marino et al., 2002) and human subjects (Carrubba et al., 2007) (Figs. 2 and 3). A typical stimulus-response relationship is shown in Figure 2, which depicts results from rat no. 1. Using $\overline{\%R(t)}$, a change in brain activity triggered by the field onset was found at 351–444 ms (29 points) by means of point-by-point comparisons between onset and control epochs ($P < 0.05$ for each pair-wise comparison in

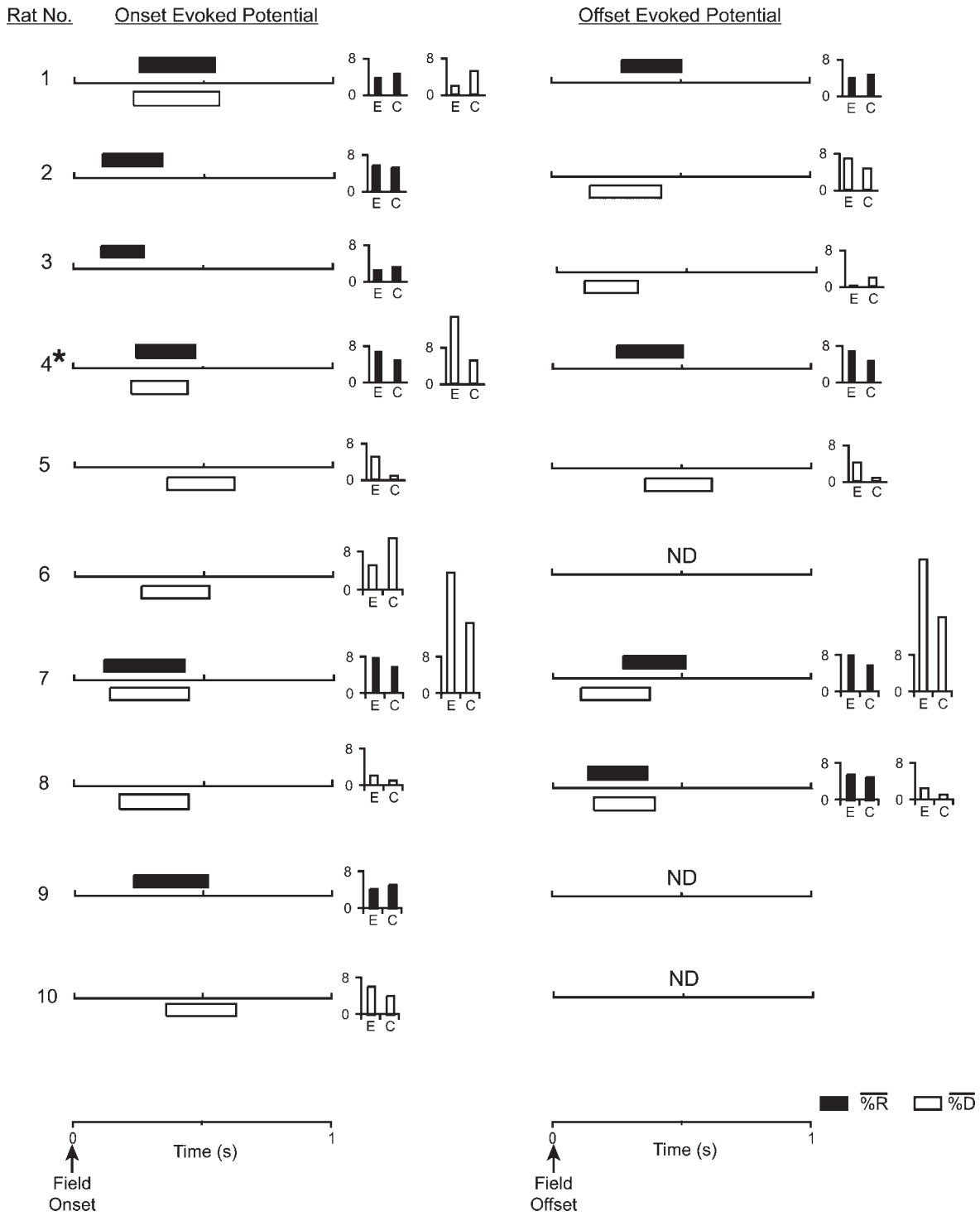

Fig. 3. Latency of onset and offset of magnetosensory evoked potentials in rats. Onset and offset magnetosensory evoked potentials shown in left and right columns, respectively. The bar graphs depict the average value of the recurrence variables in the stimulus and control epochs (E and C, respectively) for the time intervals where the epochs differed ($P < 0.05$). The SEs were not resolved at the scale shown. *False-positive detection in the onset epoch in the sham trials.

each interval) (Fig. 2a). Using $\overline{\%D}$, the effect of the field was found at 328–401 ms (23 points) (Fig. 2b). No differences in $\overline{\%R(t)}$ or $\overline{\%D(t)}$ were seen when the sham-field-onset epochs were compared with the corresponding control epochs (Figs. 2c and 2d). No significant differences between the field and control

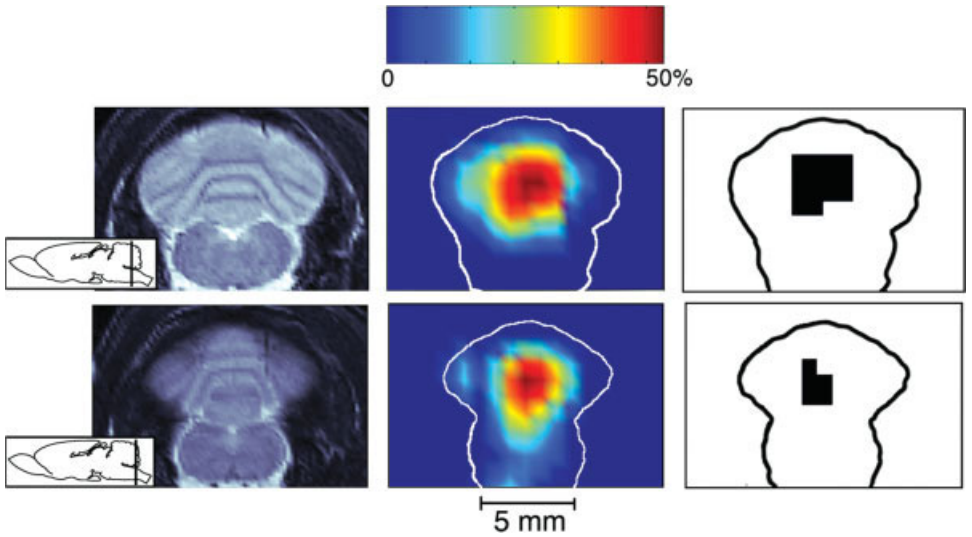

Fig. 4. Location of the magnetic-field stimulated uptake of FDG in the rat brain. The significantly activated voxels ($P < 0.05$) were located in the mid-sagittal posterior cerebellum. In the coronal plane, the activated region occurred in two consecutive PET slices (locations shown in the inserts). Column 1, coronal MRI sections of the rat brain (Schweinhardt et al., 2003); slice thickness, 1.2 mm. Column 2, average difference PET image ($n = 10$ rats). Column 3, locations (in the image plane) of the region activated by the magnetic field. Color bar for the difference image is expressed as a percent difference between the average exposure and sham-exposure PET images. The superimposed outlines are the cerebellum boundaries for each slice (from the MRI atlas).

epochs were detected in $V(t)$ when they were compared point by point (data not shown), indicating that the evoked potentials were nonlinearly related to the field.

MEPs due to field onset and/or offset were detected in all 10 rats using $\overline{\%R(t)}$ and/or $\overline{\%D(t)}$ (Fig. 3). The onset analysis for rat no. 1 (Fig. 2) was repeated to detect the effect of field offset, and both analyses were done for the other 9 rats; onset MEPs were detected in one or both recurrence quantifiers in all 10 rats, and offset MEPs were detected in 7 of the 10 rats (Fig. 3). There was one instance of a false-positive detection (sham-field onset, rat no. 4). MEPs were not detected in any rat when the EEG was analyzed by means of the method of time averaging (data not shown).

Exposure to the magnetic field stimulated cerebellar uptake of FDG (Figs. 4 and 5). We performed the PET study using another group of 10 rats and analyzed the effect of the field on FDG uptake, using an experimental design based on statistical comparison of paired samples (the same animal before and after treatment) (Figs. 4 and 5). The standard deviation of the average difference image pooled over the search volume ($V = 4088$ mm^3, $R = 511$ resels) was 28.5%, and the maximum t statistic inside the search volume was $t_{max} = 5.65$. The activated region was identified by analyzing the variance in the difference image to find the voxels for which t was greater than the critical value found from

$$P(t_{max} > t) = R(4 \log_e(2))^{3/2}(2\pi)^{-2}(t^2 - 1)e^{-t^2/2}$$

(Worsley et al., 1992). For our search volume, the critical t value was 4.65. A brain t map was constructed to identify the voxels for which $t > 4.65$, and an activated region of 15 voxels (13 mm^3) was found. The Euler characteristic was 1 with no holes in the excursion set, indicating one isolated region of activation. By comparing the location of the activated voxels in the PET image with a standard MRI of the rat brain (Schweinhardt et al., 2003), the activated region was located in the posterior central cerebellum (Figs. 4 and 5). The average increase in activation in the 15 voxels was 49%.

To confirm the reliability of the analysis, the voxel values were randomized before evaluation of the difference image. During 100 iterations of the process the critical value of 4.65 was never achieved (Fig. 6).

DISCUSSION

Previous studies had shown that low-strength EMFs produced MEPs in rabbits and human subjects, and that the stimulus-response relationship was governed by nonlinear laws. Confirmation by means of an independent method was needed to verify that EMFs affected brain activity, and to help localize the activated region. For this purpose we measured the regional rate of glucose uptake, as assessed using PET, under the assumption that the uptake would be linearly related to the electrophysiological activity triggered by the field, and hence could be detected by means of time averaging. The assumption was reasonable because glucose uptake is proportional to cell activity, unlike the electrical correlates of that activ-

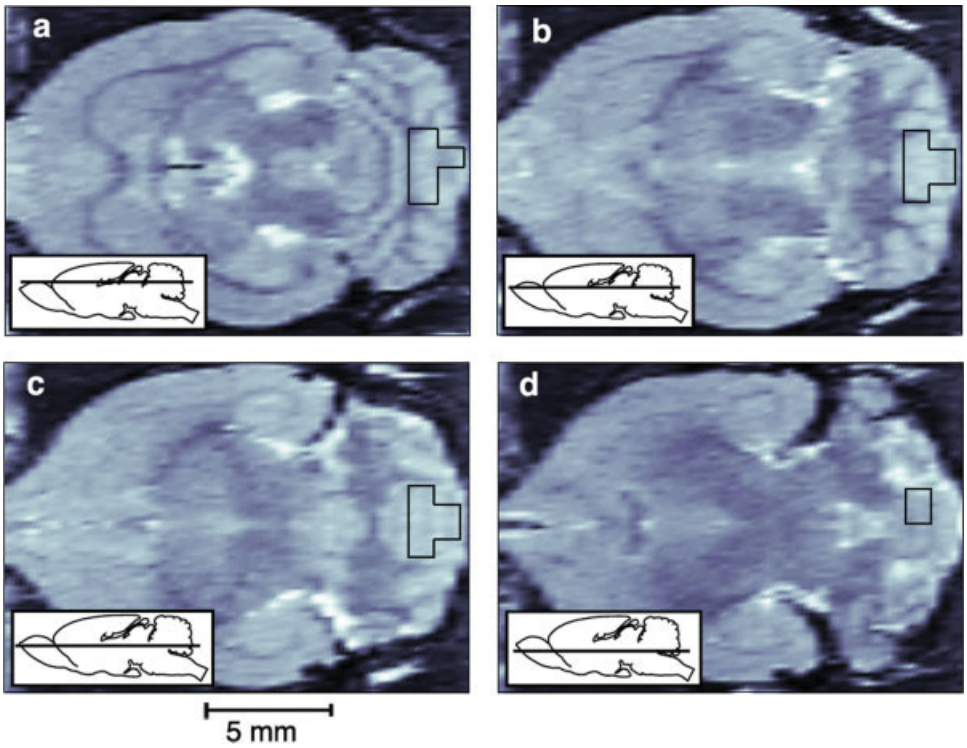

Fig. 5. Consecutive horizontal MRI atlas slices (**a–d**), 0.85 mm thick (Schweinhardt et al., 2003). Regions of statistically significant FDG uptake are outlined in black. The effect is approximately symmetric about the mid-sagittal plane of the cerebellum. [Color figure can be viewed in the online issue, which is available at www.interscience.wiley.com.]

ity which exhibited a nonlinear relationship to the field (Carrubba et al., 2007; Marino et al., 2002).

Using recurrence analysis, potentials evoked by field onset or offset or both were detected in all animals ($P < 0.05$) (Fig. 3). The potentials occurred with a latency of 100–625 ms in $V(t)$, and consisted of statistically significant increases or decreases in $\overline{\%R(t)}$ and/or $\overline{\%D(t)}$, which were the quantifiers used to capture the nonlinear determinism in $V(t)$. Several considerations indicated that the effects were true post-transduction changes in brain electrical activity triggered by the magnetic stimulus.

First, an alternative explanation that the effects resulted from an interaction between the field and the scalp electrodes can be ruled out because, in accordance with Faraday's law, such interactions begin instantaneously; in our studies they occurred within the first 30 ms after stimulus onset or offset. In contrast, the observed potentials occurred several hundred milliseconds after the stimulus, which is a typical latency for evoked potentials, for example, N200 and P300 of the auditory system (McPherson, 1996). Second, sensory evoked potentials are typically produced by both onset and offset of a stimulus but commonly more frequently in the onset epochs (Campen et al., 1997; He, 2002; Takahashi et al., 2004), and we observed similar results (Fig. 3). Third, intersubject

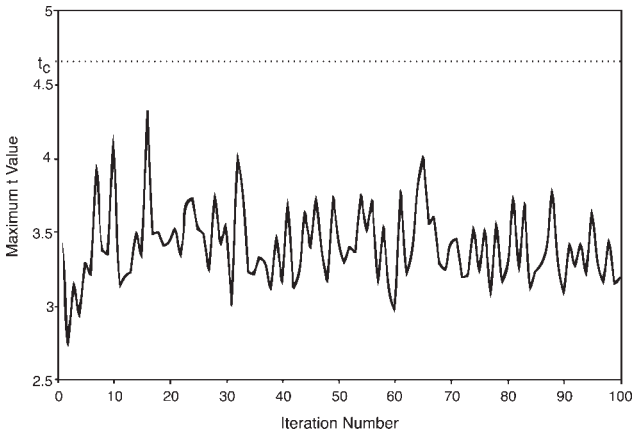

Fig. 6. Surrogate analyses of PET data. When the voxel values were randomized (100 iterations), the maximum t value was always less than the critical t value (4.65), indicating the absence of evidence of false-positive activation.

variation in latency within a reasonably well-defined range was seen, as is the case with all other known types of evoked potentials. Finally, the family-wise error rate for a decision that a rat detected a stimulus was initially estimated at $P = 0.049$, and the observed error rate based on the sham analysis was $1/20 = 0.05$ (one false-positive detection in 20 sham MEPs), empirically indicating that our statistical

decisions were reliable. It follows from all these reasons that the observed changes in brain electrical activity were true MEPs.

The MEPs were detected when $V(t)$ was analyzed by recurrence analysis but not when $V(t)$ was analyzed by time averaging. Recurrence analysis is capable of detecting linear determinism as well as nonlinear determinism (which was the application for which the technique was initially devised), whereas time averaging is capable of detecting only linear determinism (stimulus-response relationships governed by linear differential equations). Thus, taking into consideration the conditions under which we observed the MEPs as well as the mathematical properties of the techniques that we used, it can be concluded that the potentials were nonlinear in relation to the applied field.

We expect that there was postprocessing of the afferent signal that resulted from transduction of the field, and that the measured signal was the result of this processing. The situation was probably much the same as that following transduction of light, sound, or touch, as evidenced by the similarity between our latencies and those observed with the common stimuli. The observed intersubject variation in latency could have been partly due to differences in the cognitive status of the animals (Lutz et al., 2002).

A second group of rats was injected with FDG and exposed to a magnetic field under conditions such that there were 45 min $\times$ 60 s $\div$ 2 s per stimulus epoch = 1350 stimulus periods resulting in a total (onset + offset) of 2700 evoked potentials that, by hypothesis, were each accompanied by an incremental glucose uptake that did not occur in the same animal during a 45-min sham-exposure period. When the average difference uptake image was analyzed (Worsley et al., 1992), we found a single activation region of 13 mm^2 in the cerebellum ($P < 0.05$), thereby supporting the study hypothesis (Figs. 3 and 4).

Traditionally the cerebellum was associated with fine motor control (Saab and Willis, 2003), but neuroimaging techniques have shown its involvement with timing, sensory analysis, and cognition (Ioannides and Fenwick, 2005). For example, the cerebellum plays a role in the processing of somatosensory (Restuccia et al., 2007) and auditory (Petacchi et al., 2005) information, and is activated during behavioral tasks that involve time estimation (Bueti et al., 2008). Thus our imaging results (Figs. 3 and 4) are consistent with the emerging idea concerning the role of the cerebellum in the processing of sensory inputs.

The applied field was present throughout the rat's body because biological tissue is essentially transparent to magnetic fields. In principle, therefore, the electroreceptor cell could have been located anywhere in the body and the cerebellar activation we detected could have been a result of afferent signaling. Thus although our results are consistent with previous results suggesting that signal transduction occurred in the brain (Marino et al., 2003), the alternative explanation remains viable.

REFERENCES

Berg G, Spallek J, Schüz J, Schlehofer B, Böhler E, Schlaefer K, Hettinger I, Kunna-Grass K, Wahrendorf W, Blettner M, Interphone Study Group G. 2006. Occupational exposure to radio frequency/microwave radiation and the risk of brain tumors: Interphone Study Group. Germany. Am J Epidemiol 164:538–548.

Bueti D, Walsh V, Frith C, Rees G. 2008. Different brain circuits underlie motor and perceptual representations of temporal intervals. J Cogn Neurosci 20:204–214.

Carrubba S, Frilot C, Chesson A, Marino A. 2006. Detection of nonlinear event-related potentials. J Neurosci Meth 157:39–47.

Carrubba S, Frilot C, Chesson AL Jr, Marino AA. 2007. Evidence of a nonlinear human magnetic sense. Neuroscience 144:356–367.

Carrubba S, Frilot C, Chesson AL Jr, Webber CL Jr, Zbilut JP, Marino AA. 2008. Magnetosensory evoked potentials: Consistent nonlinear phenomena. Neurosci Res 60:95–105.

Eckmann J-P, Kamphorst SO, Ruelle D. 1987. Recurrence plots of dynamical systems. Europhys Lett 4:973–979.

He J. 2002. Responses in the auditory thalamus of the guinea pig. J Neurophysiol 88:2377–2386.

Ioannides AA, Fenwick PB. 2005. Imaging cerebellum activity in real time with magnetoencephalographic data. Prog Brain Res 148:139–150.

Lutz A, Lachaux JP, Martinerie J, Varela FJ. 2002. Guiding the study of brain dynamics by using first-person data: Synchrony patterns correlate with ongoing conscious states during a simple visual task. Proc Nat Acad Sci USA 99:1586–1591.

Marino AA, Nilsen E, Frilot C. 2002. Consistent magnetic-field induced changes in brain activity detected by recurrence quantification analysis. Brain Res 951:301–310.

Marino AA, Nilsen E, Frilot C. 2003. Localization of electroreceptive function in rabbits. Phys Behav 79:803–810.

McPherson DL. 1996. Late potentials of the auditory system. San Diego, CA: Singular Publishing Group, Inc.

O'Carroll MJ, Henshaw DL. 2008. Aggregating disparate epidemiological evidence: Comparing two seminal EMF reviews. Risk Anal 28:225–234.

Olden K. 1999. Health effects from exposure to power-line frequency electric and magnetic fields. National Institute of Environmental Health Sciences. NIH Publication No. 99-4493. http://www.niehs.gov/health/docs/niehs-report.pdf

Petacchi A, Laird AR, Fox PT, Bower JM. 2005. Cerebellum and auditory function: An ALE meta-analysis of functional neuroimaging studies. Hum Brain Mapp 25:118–128.

Restuccia D, Della Marca G, Valeriani M, Leggio MG, Molinari M. 2007. Cerebellar damage impairs detection of somatosensory input changes. A somatosensory mismatch-negativity study. Brain Res 130:276–287.

Saab CY, Willis WD. 2003. The cerebellum: Organization, functions and its role in nociception. Brain Res Rev 42:85–95.

Schweinhardt P, Fransson P, Olson L, Spenger C, Andersson JLR. 2003. A template for spatial normalisation of MR images of the rat brain. J Neurosci Meth 129:105–113.

Shimoji K, Ravasi L, Schmidt K, Soto-Montenegro ML, Esaki T, Seidel J, Jagoda E, Sokoloff L, Green MV, Eckelman WC. 2004. Measurement of cerebral glucose metabolic rates in the anesthetized rat by dynamic scanning with ^{18}F-FDG, the ATLAS small animal PET scanner, and arterial blood sampling. J Nucl Med 45:665–672.

Sonnier H, Marino AA. 2001. Sensory transduction as a proposed model for biological detection of electromagnetic fields. Electrobiol Magnetobiol 20:153–175.

Takahashi H, Nakao M, Kaga K. 2004. Cortical mapping of auditory-evoked offset responses in rats. Neuroreport 15:1565–1569.

Van Campen LE, Hall JW III, Grantham DW. 1997. Human offset auditory brainstem response: Effects of stimulus acoustic ringing and rise-fall time. Hearing Res 103:35–46.

Villeneuve PJ, Agnew DA, Johnson KC, Mao Y, Canadian Cancer Registries Epidemiology Research Group. 2002. Brain cancer and occupational exposure to magnetic fields among men: Results from a Canadian population-based case-control study. Int J Epidemiol 31:210–217.

Worsley KJ, Evans AC, Marrett S, Neelin P. 1992. A three-dimensional statistical analysis for CBF activation studies in human brain. J Cereb Blood Flow Metab 12:900–918.

Zbilut JP, Webber JCL. 2006. Recurrence quantification analysis. In: Akay M, editor. Wiley Encyclopedia of Biomedical Engineering. Hoboken: Wiley. p 2979–2986.